UWB Spectrally-Encoded Spread-Time CDMA in the Presence of Multiple Gaussian Interferences: RAKE Receiver and Three-Level Codes

Saeed Mashhadi and Jawad A. Salehi, *Senior Member, IEEE*

***Abstract*—In this paper we study and analyze the performance of the RAKE receiver for a typical Ultrawideband (UWB) Spectrally-Encoded Spread-Time (ST) CDMA in the presence of multiple Gaussian Interference (GI) signals. We demonstrate that by combining useful properties of three-level codes, i.e., codes with values of $-1, 0, +1$, and RAKE receiver, we can introduce a new strategy in which it can result in superior performance when compared to previous results. In particular, following a discussion on three-level codes we can show that RAKE receiver with optimum multiplicative weights achieves a better performance when compared with simple two-level codes. With the help of an example we show various properties of RAKE receiver as well as three-level codes and relate these properties to a number of simple descriptive parameters of the communication media. Simulation results obtained in this paper indicate the precision with which the analytical results have been obtained in modeling the above system.**

***Index Terms*—RAKE receiver, SNR, ST-CDMA, two- and three-level codes, UWB.**

I. Introduction

THE application of spectrally-encoded spread-time (ST) technique in ultrawideband (UWB) communications could result in significant performance improvement and brings about many fundamental and enriching principles and features. The spectrally-encoded ST technique which was first introduced in the context of optical code division multiple-access (CDMA) for femto- and pico-second light pulses [1] (extremely wideband) can be easily extended and applied to UWB nanosecond pulse systems [2]–[6].

The ability in matching the transmitted spectrum with the channel spectrum is one of the attractive features highlighted for spectrally-encoded ST technique. The direct application of spectrally-encoded ST technique to the transmission channels with disjoint or non-continuous frequency band allocation had been highlighted in [5] and [6]. This feature may prove to be an extremely important features in UWB communication systems [10]–[11] especially when it encounters multiple interferences and disjoint spectrum allocation mask, which is typical in most UWB environments [2]–[3], [12]–[13]. So from the above descriptions, it is important to highlight that the UWB migration from impulse radio to multiband schemes, due to its spectral efficiency, will remain transparent to UWB spectrally-encoded ST technique. Previously, we have reported on the advantages of applying ST to time-hopping UWB in order to combat the near-far problem while increasing the system rate and its corresponding performance [4].

In this paper we introduce and analyze an UWB spectrally-encoded ST in combating multiple Gaussian interferences while simultaneously offering multiple-access capability [7]. The superior feature in the above proposed technique is that the multiple Gaussian interference cancellation takes place by employing a RAKE detection scheme along with three-level codes, i.e., codes that can take on three values of $-1, 0, +1$ [8]. This scheme not only enhances the performance of the system but it also avoids having to design various, complex, bandpass filters for multiple Gaussian interferences removal at the receiver. In other words, we have shifted the design criterion from being a hardware oriented to an algorithmically oriented code design which can be easily implemented through software programming. We believe the technique introduced in this paper, namely UWB spectrally-encoded ST, will become an important candidate in many and various wireless communication systems.

The rest of this paper is organized as follows. In Section II we describe our system model. In Section III, we introduce the structure of RAKE receiver in the context of UWB spectrally-encoded CDMA communication systems. Section IV discusses three-level codes and compares different channel access schemes. In Section V we introduce an important and a practical example through which we show performance differences between two- and three-level codes. Furthermore in this section we present a few figures and discuss both analytical and simulation based numerical results. In fact the simulation results indicate the accuracy with which we have modeled our proposed scheme and systems. Section VI concludes the paper.

II. System Model for Two-Level Codes

In a typical ST-CDMA system each user employs a signature sequence to encode and transmit its data bits. Let $\left\{\xi_l^{(n)} : l = 1, 2, \cdots, L\right\}$ denote the random signature sequence of the nth user $(n = 1, 2, \ldots, N)$ with length L. For two-level codes the variable $\xi_l^{(n)} \in \{+1, 1\}$, and for all values of l and n the variables are mutually independent. For the nth

Paper approved by A. Zanella, the Editor for Wireless Systems of the IEEE Communications Society. Manuscript received July 7, 2006; revised March 17, 2007 and July 30, 2007. This paper is supported in part by the Iran National Science Foundation (INSF).

The authors are with the Optical Networks Research Lab (ONRL), Department of Electrical Engineering, Sharif University of Technology, Tehran 11365, Iran (e-mail: mashhadi@ee.sharif.edu, jasalehi@sharif.edu).

Digital Object Identifier 10.1109/TCOMM.2008.060285

transmitter, the signature code is constructed as

$$\xi_n(t) = \frac{\sin(\pi\Omega t)}{\pi t}\sum_{l=1}^{L}\xi_l^{(n)}\exp(j2\pi f_l t) \quad (1)$$

in which Ω is the chip bandwidth and $f_l = f_1 + (l-1)\Omega$ is the center frequency of the lth chip. Prior to transmission, $\xi_n(t)$ is convolved with $h_{tr}(t)$, the spectral shaping filter, and following the data modulation the signal $r_{tr}^{(n)}(t) = \sum_m \sum_{l=1}^{L} d_m^{(n)}\xi_l^{(n)}p_{tr}^{(l)}(t - mT_b)$ is transmitted through the channel. Here we can define the equivalent lth frequency chip transmitted pulse shape as $p_{tr}^{(l)}(t) = h_{tr}(t) * \frac{\sin(\pi\Omega t)}{\pi t}\exp(j2\pi f_l t)$. In our communication system $d_m^{(n)} \in \{+1,-1\}$ is equiprobable, independent, and identically distributed (i.i.d) binary information bit at the mth signaling interval with T_b denoting the bit duration. From the above definitions the total signal bandwidth transmitted into the channel is equal to $W = L\Omega$.

At the receiver end $r_{tr}^{(n)}$ is affected by delay, multipath phase degradation, fading attenuation and channel impulse response $h_{ch}(t)$ and we obtain

$$r_{rec}^{(n)}(t) = \sum_m \sum_{l=1}^{L}\sum_{k=1}^{K} d_m^{(n)}\xi_l^{(n)}\alpha_{l,k}^{(n,m)}\exp\left(j\theta_{l,k}^{(n,m)}\right) p_{rec}^{(l)}\left(t - mT_b - \tau_n - \tau_{l,k}^{(n,m)}\right) \quad (2)$$

in which $p_{rec}^{(l)}(t) = p_{tr}^{(l)}(t) * h_{ch}(t)$ is the equivalent received pulse shape for the lth frequency chip $\alpha_{l,k}^{(n,m)}, \theta_{l,k}^{(n,m)}$, and $\tau_{l,k}^{(n,m)}$ denote fading power coefficients, multipath phases, and delay coefficients respectively. All of the above parameters are functions of the nth user, lth frequency chip position, kth path number, and the mth signaling interval. We assume that all of the above random variables are mutually independent with distributions specified by the properties of channel under consideration. Furthermore, τ_n denotes the nth user's random time delay which is assumed to be independent of all other variables of the communication media and is uniformly distributed on $[0, T_b]$. In the following, we assume that the receiver has a complete prior knowledge on $h(t) = h_{tr}(t) * h_{ch}(t)$. In the presence of multiple Gaussian interference the received signal at the front end of the receiver is as follows;

$$r(t) = \sum_{n=1}^{N} r_{rec}^{(n)}(t) + \sum_{l=1}^{L} J_l(t) + n(t) \quad (3)$$

In (3) $J_l(t)$ denotes the zero mean Gaussian Interference (GI) with power spectral density (PSD) N_l^{GI} over the entire bandwidth of the lth frequency chip position, i.e., $f_l - \Omega/2 \leq f \leq f_l + \Omega/2$, and $n(t)$ denotes Additive White Gaussian Noise (AWGN) with PSD N_0. In case of no interference on a frequency chip position, we set the corresponding value of N_l^{GI} to zero. We assume independent interferences, perfect synchronization between any transmitter-receiver pairs, and denote the first user as our desired user, i.e., $n = 1$. Hence, we set $\tau_1 = 0$ and design a receiver that extracts $d_0^{(1)}$ the information bit of the $0th$ signaling interval of the first user.

III. RAKE Receiver Structure for Two-Level Codes

We consider a RAKE receiver with $L \times K$ branches. The output for the $\widehat{l}th$ frequency chip position of the $\widehat{k}th$ path is given by

$$r_{\widehat{l},\widehat{k}} = \int_{-\infty}^{+\infty} r(t) \times \left[\xi_{\widehat{l}}^{(1)}\exp\left(-j\theta_{\widehat{l},\widehat{k}}^{(1,0)}\right)p_{rec}^{(\widehat{l})*}\left(t - \tau_{\widehat{l},\widehat{k}}^{(1,0)}\right)\right]dt$$
$$\widehat{l} = 1,2,\ldots,L, \widehat{k} = 1,2,\ldots,K. \quad (4)$$

Where $*$ denotes complex conjugate operation. Appendix A verifies that $r_{\widehat{l},\widehat{k}}$s have the following general form of

$$r_{\widehat{l},\widehat{k}} = d_0^{(1)}\alpha_{\widehat{l},\widehat{k}}^{(1,0)}E_{\widehat{l}} + n_{\widehat{l},\widehat{k}}^{MPI} + n_{\widehat{l},\widehat{k}}^{MAI} + n_{\widehat{l},\widehat{k}}^{GI} + n_{\widehat{l},\widehat{k}}^{AWGN} \quad (5)$$

in which $\alpha_{\widehat{l},\widehat{k}}^{(1,0)}E_{\widehat{l}}$, $n_{\widehat{l},\widehat{k}}^{MPI}$, $n_{\widehat{l},\widehat{k}}^{MAI}$, $n_{\widehat{l},\widehat{k}}^{GI}$, and $n_{\widehat{l},\widehat{k}}^{AWGN}$ are the received energy and interfering variables on the $\widehat{l}th$ frequency chip position of $\widehat{k}th$ path. In the above equation we have five different terms indicating first the desired information bit term, multipath interference term (MPI), multiple-access interference term (MAI), Gaussian interference term (GI), and additive white Gaussian noise term (AWGN).

If we define $g'_{\widehat{l},\widehat{k}}$ as the gain coefficient used at the receiver for the $\widehat{l}th$ frequency chip and the $\widehat{k}th$ path, then its optimum value can be represented as (6) (see next page), where η_k, $\eta'_{k,\widehat{k}}$, and $\eta''_{k,\widehat{k}}$ are defined in Appendix A. Including the first user's signature sequence and the multipath phases then the equivalent total gain in $\widehat{l}th$ chip and $\widehat{k}th$ path position of the receiver is $g_{\widehat{l},\widehat{k}} = \xi_{\widehat{l}}^{(1)}\exp\left(-j\theta_{\widehat{l},\widehat{k}}^{(1,0)}\right)g'_{\widehat{l},\widehat{k}}$. Using (6) we obtain the final value for the decision variable as $r = \sum_{\widehat{l}=1}^{L}\sum_{\widehat{k}=1}^{K} g'_{\widehat{l},\widehat{k}} \times r_{\widehat{l},\widehat{k}}$. At the receiver we decide on $d_0^{(1)} = +1$ if $r \geq 0$ and $d_0^{(1)} = -1$ if $r < 0$. The final structure of this receiver is depicted in Fig. 1. Prior to any further discussion, it is interesting to note (7) (see next page). Based on the above equation, the final structure of the RAKE receiver is a correlator using the signal $h(t) * \sum_{\widehat{l}=1}^{L}\sum_{\widehat{k}=1}^{K} g_{\widehat{l},\widehat{k}}\exp\left(-j2\pi f_{\widehat{l}}\left(t - \tau_{\widehat{l},\widehat{k}}^{(1,0)}\right)\right)\frac{\sin\left(\pi\Omega\left(t-\tau_{\widehat{l},\widehat{k}}^{(1,0)}\right)\right)}{\pi\left(t-\tau_{\widehat{l},\widehat{k}}^{(1,0)}\right)}$ as its multiplicative signal.

The derivation of the exact expression of the probability of error for the above system could be tedious and difficult and hence we resort to Gaussian approximation. However, we note that all four variables $n_{\widehat{l},\widehat{k}}^{MPI}$, $n_{\widehat{l},\widehat{k}}^{MAI}$, $n_{\widehat{l},\widehat{k}}^{GI}$ and $n_{\widehat{l},\widehat{k}}^{AWGN}$ are uncorrelated, $n_{\widehat{l},\widehat{k}}^{GI}$ and $n_{\widehat{l},\widehat{k}}^{AWGN}$ are Gaussian and $n_{\widehat{l},\widehat{k}}^{MPI}$ and $n_{\widehat{l},\widehat{k}}^{MAI}$ have distributions that are very close to the Gaussian distribution for moderate values of K, please see Appendix A for details. This interesting superiority of ST-CDMA over other CDMA techniques, specifically in UWB communications with a high number of resolvable paths, is also reported in [4]–[5]. Therefore, we can expect that Gaussian approximation obtains results which are close to the exact value of PE. If we define conditional SNR for the two-level codes as (8), and assume that $\alpha_{l,k}^{(n,m)}$s have Nakagami

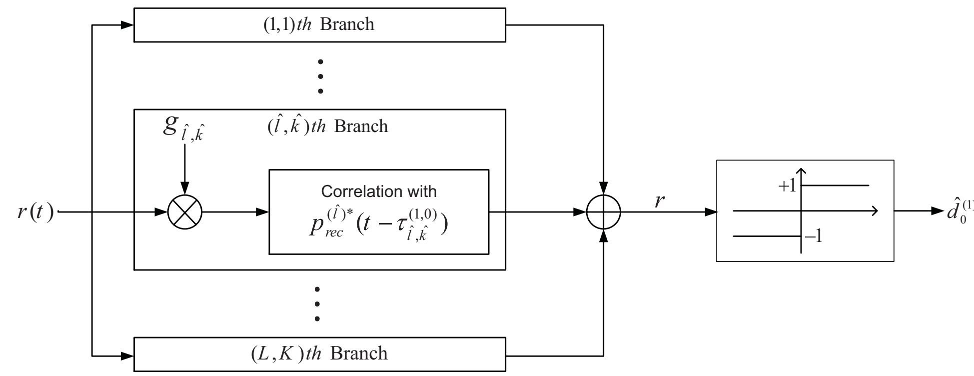

Fig. 1. Final structure of receiver.

$$g'_{\widehat{l},\widehat{k}}=\frac{\alpha_{\widehat{l},\widehat{k}}^{(1,0)}}{\left(\sum_{\substack{k=1\\k\neq\widehat{k}}}^{K}\eta_k\eta'_{k,\widehat{k}}+2\left(N-1\right)\sum\limits_{k=1}^{K}\eta_k\eta''_{k,\widehat{k}}\right)E_{\widehat{l}}+N_{\widehat{l}}^{GI}+N_0} \tag{6}$$

$$r=\int\limits_{-\infty}^{+\infty}r\left(t\right)\times\left(h\left(t\right)*\sum_{\widehat{l}=1}^{L}\sum_{\widehat{k}=1}^{K}g_{\widehat{l},\widehat{k}}\exp\left(-j2\pi f_{\widehat{l}}\left(t-\tau_{\widehat{l},\widehat{k}}^{(1,0)}\right)\right)\frac{\sin\left(\pi\Omega\left(t-\tau_{\widehat{l},\widehat{k}}^{(1,0)}\right)\right)}{\pi\left(t-\tau_{\widehat{l},\widehat{k}}^{(1,0)}\right)}\right)dt \tag{7}$$

$$SNR_{two-level}^{cond.}=\sum_{\widehat{l}=1}^{L}\sum_{\widehat{k}=1}^{K}\frac{\left(\alpha_{\widehat{l},\widehat{k}}^{(1,0)}\right)^2E_{\widehat{l}}}{\left(\sum_{\substack{k=1\\k\neq\widehat{k}}}^{K}\eta_k\eta'_{k,\widehat{k}}+2\left(N-1\right)\sum\limits_{k=1}^{K}\eta_k\eta''_{k,\widehat{k}}\right)E_{\widehat{l}}+N_{\widehat{l}}^{GI}+N_0} \tag{8}$$

distribution with parameters μ_k and η_k, i.e.,

$$P\left(\alpha\right)=\frac{2\alpha^{2\mu_k-1}}{\Gamma\left(\mu_k\right)}\left(\frac{\mu_k}{\eta_k}\right)^{\mu_k}\exp\left(-\frac{\mu_k}{\eta_k}\alpha^2\right)\quad\alpha\geq0 \tag{9}$$

then the conditional probability of error can be expressed as $PE_{two-level}^{cond.}=Q\left(\sqrt{2SNR_{two-level}^{cond.}}\right)$, in which $\Gamma\left(x\right)=\int\limits_0^\infty t^{x-1}e^{-t}dt$ and $Q\left(x\right)=\frac{1}{\sqrt{2\pi}}\int\limits_x^\infty e^{-t^2/2}dt$. In order to find $PE_{two-level}$, it can be seen that $SNR_{two-level}^{cond.}$ has the following moment generating function (MGF) as (10) (see top of next page), with $\mathbf{E}$ denoting the expectation operation. Thus finding the probability distribution and consequently averaging over $PE_{two-level}^{cond.}$, in general, is a tedious and unyielding task and can only be obtained numerically for the special cases under consideration. However, in Section V, we will consider an important and yet a simple and a viable example in which through some practical assumptions we can obtained an analytical solution for $PE_{two-level}$.

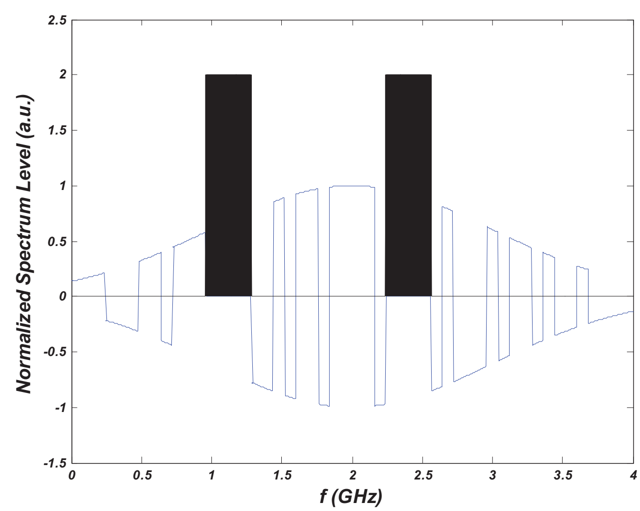

Fig. 2. Signal and interferences spectrum. In this figure we have two interferences shown by blocks of solid black.

IV. THREE LEVEL CODES

In the previous section we discussed the RAKE receiver structure for a typical UWB ST-CDMA communication system in the presence of multiple Gaussian interferences. It is shown that under the assumption of using two-level codes, we need to use the content of the whole frequency band of the received signal $r\left(t\right)$ in order to achieve the minimum error. However, in this section we use three-level codes, i.e., $\xi_l^{(1)}\in\{-1,0,+1\}$, instead of the simple two-level codes or $\xi_l^{(1)}\in\{-1,+1\}$. In Fig. 2. we sketch a typical spectrum of three-level coded signal in the presence of two Gaussian interferences.

The obvious question, hence, is whether we can design and employ three-level codes such that we can obtain a better performance when compared with employing two-level codes? In other words, how should we select zero elements of a three-level code and their positions in the sequence in order to have

$$\mathbf{E}\left(\exp\left(s \times SNR_{two-level}^{cond.}\right)\right) = \prod_{\widehat{l}=1}^{L}\prod_{\widehat{k}=1}^{K}\left(\begin{array}{c} 1-\left[E_{\widehat{l}}\sum_{\substack{k=1\\k\neq\widehat{k}}}^{K}\eta_k\eta'_{k,\widehat{k}} + 2\left(N-1\right)E_{\widehat{l}}\sum_{k=1}^{K}\eta_k\eta''_{k,\widehat{k}} + N_{\widehat{l}}^{GI} + N_0\right]^{-1} \\ \times\left(E_{\widehat{l}}\eta_{\widehat{k}}/\mu_{\widehat{k}}\right)\times s \end{array}\right)^{-\mu_k} \quad (10)$$

the best performance? In fact, by using three-level codes, one can select a more elaborated approach to use the available bandwidth. For example, for the best performance, one can examine different frequency slots and sort them in the order of their ability to safely transmit data and then decide on the usefulness or uselessness of each frequency slot in the code construction.

Clearly there are some trade-offs in applying this strategy that need to be considered in detail. Indeed, under the constant average power assumption (equivalent to $E = cte.$), using better frequency slots only, i.e., frequency slots with no interference, the transmitter-receiver pairs reduce (or probably completely remove) the effect of the interferences on their decision variable. But on the other hand the cost is the lower overall multiple-access processing gain, i.e., code length, which may degrade the overall probability of error. This idea suggests that there is an optimum solution that not only minimizes the interference effect but also uses the total bandwidth in the best possible allowable scheme for multiple users.

A. Known Fading Coefficients

Here, we have two different scenarios related to prior knowledge or absolutely no knowledge on the value of fading coefficients $\alpha_{l,k}^{(n,m)}$. At first we consider the case that perfect knowledge on the fading coefficients is available for both transmitter and receiver. As a result we can define the SNR conditioned on $\widehat{l}th$ frequency chip as (11) (see top of next page).

Without any loss of generality, assume $SNR_1^{cond.} \geq SNR_2^{cond.} \geq \ldots \geq SNR_L^{cond.}$. Since the probability of error depends only on $SNR_{three-level}^{cond.} = \sum_{\widehat{l}} SNR_{\widehat{l}}^{cond.}$ and also since for all $\widehat{l}$, $SNR_{\widehat{l}}^{cond.} \geq 0$, it is clear that zero valued chip positions may be selected from the end positions to the starting positions of multiple-access codes. Hence, by denoting the number of zero valued frequency chip positions as L_{zero}, then the total energy gain on the nonzero frequency chips or slots will be equal to $g = \frac{\sum_{\widehat{l}=1}^{L} E_{\widehat{l}}}{\sum_{\widehat{l}=1}^{L-L_{zero}} E_{\widehat{l}}} = \frac{E}{\sum_{\widehat{l}=1}^{L-L_{zero}} E_{\widehat{l}}} \geq 1$. Thus we find the conditional SNR for the three-level codes as (12) (see next page).

Equation (12) clearly shows the trade-off between the small and the large values of L_{zero}. Since maximizing SNR is equivalent to the minimizing probability of error, the optimum value of L_{zero} is that value which maximizes (12). Obviously, in finding the optimum value we require the knowledge of all the parameters in (12), which depends on the specific problem under consideration. After determining L_{zero}, both transmitter and receiver agree on using the frequency chips with tag number $\widehat{l} = 1, 2, \ldots, L - L_{zero}$. In the following section we show that with this strategy in mind we can obtain $SNR_{three-level}$ such that $PE_{three-level} \leq PE_{two-level}$, hence a more elaborate use of the available bandwidth. It is obvious that the improvement caused by using three-level codes over simple two-level codes is much noticeable in high interference regimes as it can be seen in the example presented in the next section.

B. Unknown Fading Coefficients

Although having the information on the fading coefficients at the transmitter is valuable, it is not the case in many applications due to some complexities such as the need to have a reverse channel, error in finding true values at the transmitter, the need to have a more complex online system at both transmitter and receiver end, and the possibility of fast channel changes. Here, we can use a simplified version of the previous SNR expression. To this end, let us define the average $\widehat{l}th$ frequency chip SNR as (13) (see next page). $SNR_{\widehat{l}}$ is simply the average value of $SNR_{\widehat{l}}^{cond.}$ given in (11) and can be obtained without any need to the prior knowledge of the actual value of $\alpha_{l,k}^{(n,m)}$. These properties suggest that we can reasonably use $SNR_{\widehat{l}}$s instead of $SNR_{\widehat{l}}^{cond.}$s to quantify for different frequency chips or slots. $SNR_{\widehat{l}}$s not only are simple, direct and meaningful measures, but also can be used in both transmitter and receiver without the need to a complex bidirectional system. The remaining part of the procedure in unknown fading coefficient case is similar to the previous case.

V. Discussions and Important Example

The analytical expressions on the error rate for the two- and the three-level codes are given in this section and, through a simple but yet a very practical example, their differences in performance are also illustrated. It is obvious that for a fair comparison, we need to examine both cases under the same scenarios and therefore we only consider the case of unknown fading coefficients at the transmitter.

The example: Assume the case of

$$E_l = E/L$$

and

$$N_l^{GI} = \begin{cases} N_{GI} & L - L_{GI} + 1 \leq l \leq L \\ 0 & otherwise \end{cases},$$

in which L_{GI} is the number of frequency chips or slots that are affected by Gaussian interferences. Furthermore, assume that $\eta_k/\mu_k = \rho$ is independent of k, which is a practical and simplifying approximation introduced in [7].

To find an analytic solution, we use certain simplifying relations. In Appendix B we show that $\eta'_{k,\widehat{k}} \cong 1$ and $\eta''_{k,\widehat{k}} \cong \frac{1}{2\Omega T_b}$ and hence (8) simplifies into (14) (see next page). Here, by

$$SNR_{\hat{l}}^{cond.} = \sum_{\hat{k}=1}^{K} \frac{\left(\alpha_{\hat{l},\hat{k}}^{(1,0)}\right)^2 E_{\hat{l}}}{\left(\sum_{\substack{k=1\\k\neq\hat{k}}}^{K} \eta_k \eta'_{k,\hat{k}} + 2(N-1)\sum_{k=1}^{K} \eta_k \eta''_{k,\hat{k}}\right) E_{\hat{l}} + N_{\hat{l}}^{GI} + N_0} \tag{11}$$

$$SNR_{three-level}^{cond.} = \sum_{\hat{l}=1}^{L-L_{zero}} \sum_{\hat{k}=1}^{K} \frac{\left(\alpha_{\hat{l},\hat{k}}^{(1,0)}\right)^2 E_{\hat{l}}}{\left(\sum_{\substack{k=1\\k\neq\hat{k}}}^{K} \eta_k \eta'_{k,\hat{k}} + 2(N-1)\sum_{k=1}^{K} \eta_k \eta''_{k,\hat{k}}\right) E_{\hat{l}} + \left(N_{\hat{l}}^{GI} + N_0\right) \times \sum_{\hat{l}=1}^{L-L_{zero}} \frac{E_l}{E}} \tag{12}$$

$$SNR_{\hat{l}} = \sum_{\hat{k}=1}^{K} \frac{\eta_{\hat{k}} E_{\hat{l}}}{\left(\sum_{\substack{k=1\\k\neq\hat{k}}}^{K} \eta_k \eta'_{k,\hat{k}} + 2(N-1)\sum_{k=1}^{K} \eta_k \eta''_{k,\hat{k}}\right) E_{\hat{l}} + N_{\hat{l}}^{GI} + N_0} \tag{13}$$

$$\begin{aligned} SNR_{two-level}^{cond.} &= \sum_{\hat{l}=1}^{L} \sum_{\hat{k}=1}^{K} \frac{\frac{E}{L}\left(\alpha_{\hat{l},\hat{k}}^{(1,0)}\right)^2}{\frac{E}{L}\left(\sum_{\substack{k=1\\k\neq\hat{k}}}^{K} \eta_k + \frac{(N-1)}{\Omega T_b}\sum_{k=1}^{K} \eta_k\right) + N_{\hat{l}}^{GI} + N_0} \\ &\cong \frac{\frac{E}{L}\sum_{\hat{l}=1}^{L-L_{GI}} \sum_{\hat{k}=1}^{K}\left(\alpha_{\hat{l},\hat{k}}^{(1,0)}\right)^2}{\frac{E}{L}\left(1+\frac{(N-1)}{\Omega T_b}\right)\sum_{k=1}^{K}\eta_k + N_0} + \frac{\frac{E}{L}\sum_{\hat{l}=L-L_{GI}+1}^{L} \sum_{\hat{k}=1}^{K}\left(\alpha_{\hat{l},\hat{k}}^{(1,0)}\right)^2}{\frac{E}{L}\left(1+\frac{(N-1)}{\Omega T_b}\right)\sum_{k=1}^{K}\eta_k + N_{GI} + N_0} \end{aligned} \tag{14}$$

denoting

$$\gamma_1 = \frac{\frac{2E}{L}\sum_{\hat{l}=1}^{L-L_{GI}} \sum_{\hat{k}=1}^{K}\left(\alpha_{\hat{l},\hat{k}}^{(1,0)}\right)^2}{\frac{E}{L}\left(1+\frac{(N-1)}{\Omega T_b}\right)\sum_{k=1}^{K}\eta_k + N_0} \tag{15a}$$

$$\gamma_2 = \frac{\frac{2E}{L}\sum_{\hat{l}=L-L_{GI}+1}^{L} \sum_{\hat{k}=1}^{K}\left(\alpha_{\hat{l},\hat{k}}^{(1,0)}\right)^2}{\frac{E}{L}\left(1+\frac{(N-1)}{\Omega T_b}\right)\sum_{k=1}^{K}\eta_k + N_{GI} + N_0} \tag{15b}$$

then $PE_{two-level} = \int_0^\infty \int_0^\infty Q\left(\sqrt{\gamma_1+\gamma_2}\right) P(\gamma_1) P(\gamma_2)\, d\gamma_1 d\gamma_2$, in which $P(\gamma_1)$ and $P(\gamma_2)$ are obtained in Appendix C and are expressed as (16) (see next page). Similarly, for the three-level codes we have (17) (see next page), and by defining (18a) and (18b) (see next page), we can find $PE_{three-level} = \int_0^\infty \int_0^\infty Q\left(\sqrt{\gamma_1+\gamma_2}\right) P(\gamma_1) P(\gamma_2)\, d\gamma_1 d\gamma_2$, with $P(\gamma_1)$ and $P(\gamma_2)$ obtained in Appendix C and are expressed as (19) (see next page).

First of all in order to compare the two coding schemes we need to find the optimum value for L_{zero}. In order to obtain the optimum value of L_{zero} one needs to minimize $PE_{three-level}$. However due to unyielding minimization we can resort, to a good degree of accuracy, in maximizing the expected SNR value. Hence, we can write (20).

We obtain the optimum value for L_{zero} by maximizing (20). Following some algebraic manipulations and using the fact that $0 \le L_{zero} \le L_{GI}$ we can obtain the optimum value for L_{zero}, denoted by $L_{zero,optimum}$ as (21), in which $c_1 = \frac{L-L_{GI}}{L}$, $c_2 = \frac{N_{GI}}{N_0}$, $PG_1 = \frac{\rho E}{L N_0}$, $PG_2 = L\sum_{k=1}^{K}\mu_k$, $PG_3 = \frac{L}{1+(N-1)/\Omega T_b}$, and $c_3 = \frac{PG_1 \times PG_2}{PG_3}$. In this example, the final value of PE, for two- or three-level codes, is a function of five different parameters, namely, c_1; the parameter representing the effect of Gaussian interference bandwidth, c_2; the parameter representing the effect of Gaussian interference power, $PG_1 = \frac{\rho E}{L N_0}$; the parameter representing

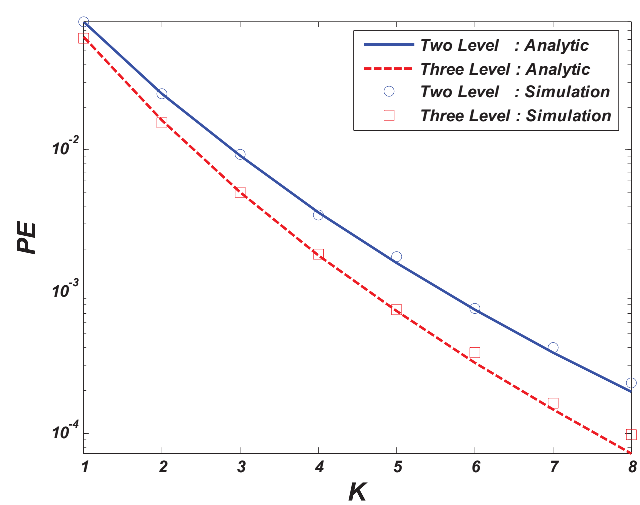

Fig. 3. $PE_{two-level}$ and $PE_{three-level}$ versus K for $L = 120, c_1 = 0.8, c_2 = 100, PG_1 = 0.25, PG_2 = 36, PG_3 = 30$.

$$\begin{aligned} P(\gamma_1) &= \frac{1/\gamma_1}{\Gamma\left((L-L_{GI})\sum_{k=1}^{K}\mu_k\right)} \times (\gamma_1/\rho\rho_1)^{(L-L_{GI})\sum_{k=1}^{K}\mu_k} \times \exp(-\gamma_1/\rho\rho_1) \\ P(\gamma_2) &= \frac{1/\gamma 2}{\Gamma\left(L_{GI}\sum_{k=1}^{K}\mu_k\right)} \times (\gamma_2/\rho\rho_2)^{L_{GI}\sum_{k=1}^{K}\mu_k} \times \exp(-\gamma_2/\rho\rho_2) \end{aligned} \tag{16}$$

$$\begin{aligned} SNR_{three-level}^{cond.} \cong & \frac{\frac{E}{L}\sum_{\widehat{l}=1}^{L-L_{GI}}\sum_{\widehat{k}=1}^{K}\left(\alpha_{\widehat{l},\widehat{k}}^{(1,0)}\right)^2}{\frac{E}{L}\left(1+\frac{(N-1)}{\Omega T_b}\right)\sum_{k=1}^{K}\eta_k + N_0\times(1-L_{zero}/L)} \\ & + \frac{\frac{E}{L}\sum_{\widehat{l}=L-L_{GI}+1}^{L-L_{zero}}\sum_{\widehat{k}=1}^{K}\left(\alpha_{\widehat{l},\widehat{k}}^{(1,0)}\right)^2}{\frac{E}{L}\left(1+\frac{(N-1)}{\Omega T_b}\right)\sum_{k=1}^{K}\eta_k + (N_{GI}+N_0)\times(1-L_{zero}/L)} \end{aligned} \tag{17}$$

$$\gamma_1' = \frac{\frac{2E}{L}\sum_{\widehat{l}=1}^{L-L_{GI}}\sum_{\widehat{k}=1}^{K}\left(\alpha_{\widehat{l},\widehat{k}}^{(1,0)}\right)^2}{\frac{E}{L}\left(1+\frac{(N-1)}{\Omega T_b}\right)\sum_{k=1}^{K}\eta_k + N_0\times(1-L_{zero}/L)} \tag{18a}$$

$$\gamma_2' = \frac{\frac{2E}{L}\sum_{\widehat{l}=L-L_{GI}+1}^{L-L_{zero}}\sum_{\widehat{k}=1}^{K}\left(\alpha_{\widehat{l},\widehat{k}}^{(1,0)}\right)^2}{\frac{E}{L}\left(1+\frac{(N-1)}{\Omega T_b}\right)\sum_{k=1}^{K}\eta_k + (N_{GI}+N_0)\times(1-L_{zero}/L)} \tag{18b}$$

$$\begin{aligned} P(\gamma_1') &= \frac{1/\gamma_1'}{\Gamma\left((L-L_{GI})\sum_{k=1}^{K}\mu_k\right)} \times (\gamma_1'/\rho\rho_1')^{(L-L_{GI})\sum_{k=1}^{K}\mu_k} \times \exp(-\gamma_1'/\rho\rho_1') \\ P(\gamma_2') &= \frac{1/\gamma_2'}{\Gamma\left((L_{GI}-L_{zero})\sum_{k=1}^{K}\mu_k\right)} \times (\gamma_2'/\rho\rho_2')^{(L_{GI}-L_{zero})\sum_{k=1}^{K}\mu_k} \times \exp(-\gamma_2'/\rho\rho_2') \end{aligned} \tag{19}$$

$$\begin{aligned} SNR_{three-level} &= \mathbf{E}\left(SNR_{three-level}^{cond.}\right) \\ &= \frac{(L-L_{GI})\times\frac{E}{L}\sum_{k=1}^{K}\eta_k}{\frac{E}{L}\left(1+\frac{(N-1)}{\Omega T_b}\right)\sum_{k=1}^{K}\eta_k + N_0\times(1-L_{zero}/L)} \\ &\quad + \frac{(L_{GI}-L_{zero})\times\frac{E}{L}\sum_{k=1}^{K}\eta_k}{\frac{E}{L}\left(1+\frac{(N-1)}{\Omega T_b}\right)\sum_{k=1}^{K}\eta_k + (N_{GI}+N_0)\times(1-L_{zero}/L)} \end{aligned} \tag{20}$$

$$\frac{L_{zero,optimum}}{L} = \begin{cases} 0 & \frac{c_3+c_2\sqrt{c_1(c_1+c_3+c_1c_2)}}{c_1c_2(1+c_2)-c_3}\times c_3 < 0 \\ 1-c_1 & 0 < \frac{c_3+c_2\sqrt{c_1(c_1+c_3+c_1c_2)}}{c_1c_2(1+c_2)-c_3}\times c_3 \le c_1 \\ 1-\frac{c_3+c_2\sqrt{c_1(c_1+c_3+c_1c_2)}}{c_1c_2(1+c_2)-c_3}\times c_3 & c_1 \le \frac{c_3+c_2\sqrt{c_1(c_1+c_3+c_1c_2)}}{c_1c_2(1+c_2)-c_3}\times c_3 \le 1 \\ 0 & 1 \le \frac{c_3+c_2\sqrt{c_1(c_1+c_3+c_1c_2)}}{c_1c_2(1+c_2)-c_3}\times c_3 \end{cases} \tag{21}$$

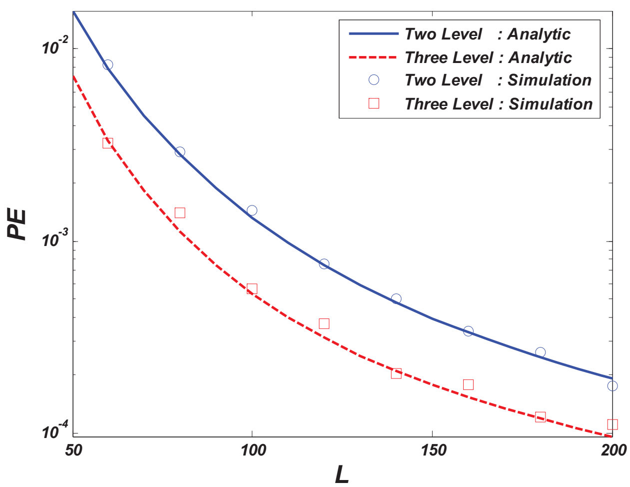

Fig. 4. $PE_{two-level}$ and $PE_{three-level}$ versus L for $K=6, L_{GI}=24, c_2=100, PG_1=0.25, PG_2=36, PG_3=30$.

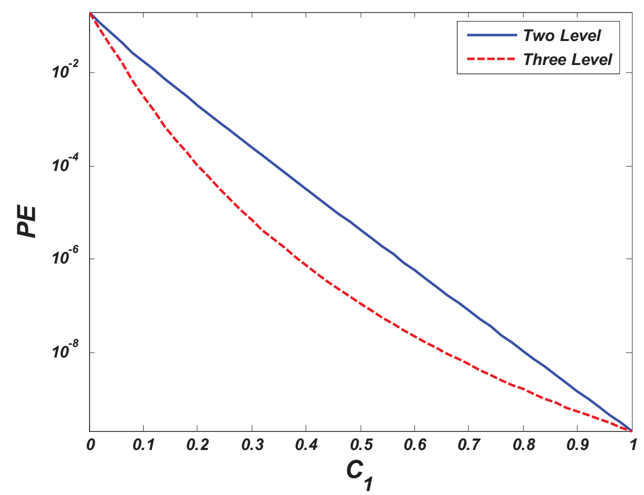

Fig. 6. $PE_{two-level}$ and $PE_{three-level}$ versus c_1 for $c_2=100, PG_1=0.5, PG_2=72, PG_3=60$.

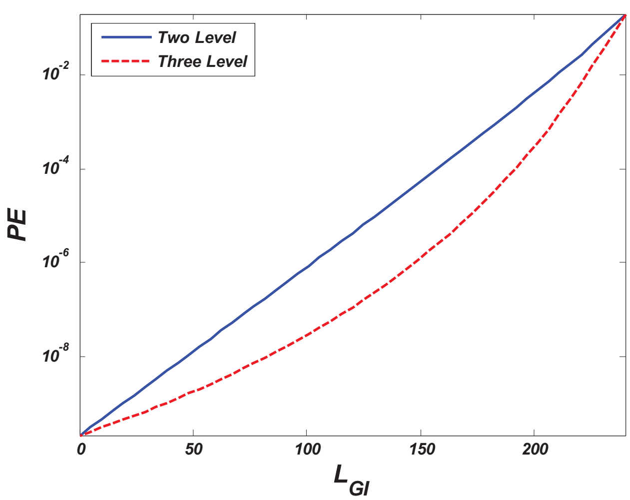

Fig. 5. $PE_{two-level}$ and $PE_{three-level}$ versus L_{GI} for $c_2=100, PG_1=0.5, PG_2=72, PG_3=60$.

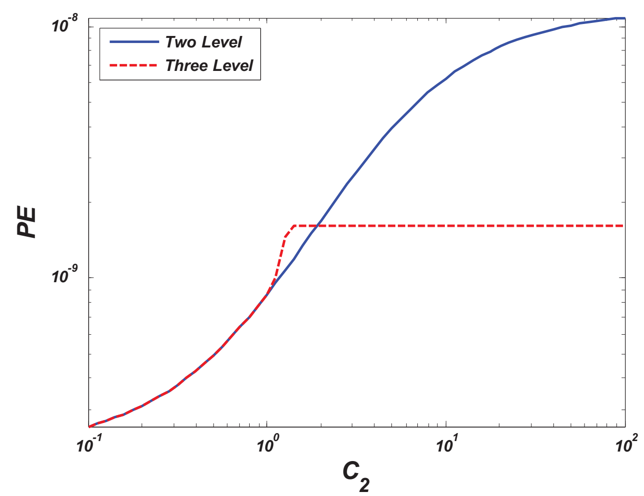

Fig. 7. $PE_{two-level}$ and $PE_{three-level}$ versus c_2 for $c_1=0.8, PG_1=0.5, PG_2=72, PG_3=60$.

signal-to-noise power ratio processing gain, $PG_2 = L\sum_{k=1}^{K}\mu_k$; the parameter representing multichannel processing gain and it is proportional to $L\times K$ which is the intrinsic processing gain of a typical multiband-multipath channel, and $PG_3 = \frac{L}{1+(N-1)/\Omega T_b}$; the parameter representing code length processing gain including the effect of multiple-access and multipath interferences. In the following figures we sketch PE versus different design conditions, i.e., different values of $c_1, c_2, PG_1, PG_2, PG_3$ with the optimum value of L_{zero}, i.e., $L_{zero,optimum}$, for the three-level codes obtained from (21). We can observe from Figs. 3-10 that the three-level codes system outperforms the two-level codes system. In these figures we assume that $\Omega T_b = 2$ and the Nakagami parameters are $\rho = 0.5$ and $\mu_k = 0.05$ for all values of k. Figs. 3 and 4 show that using three-level codes in all scenarios will result in a better performance than the two-level codes. In contrast in Fig. 5 three-level codes can be helpful only for moderate values of L_{GI}. Furthermore, in Figs. 3 and 4 we sketched the simulation results which indicate the precision with which the analytical results have been obtained.

Fig. 6 shows that in the case of very narrow ($c_1 \to 1$) or very wideband ($c_1 \to 0$) interference, the improvement obtained by using three-level codes is limited. But, for moderate

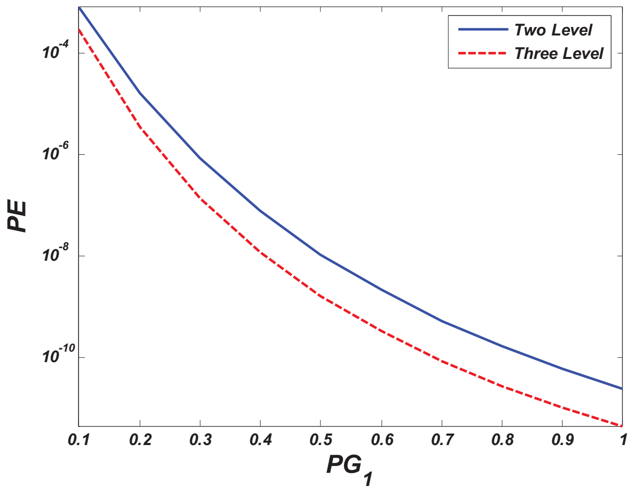

Fig. 8. $PE_{two-level}$ and $PE_{three-level}$ versus PG_1 for $c_1 = 0.8, c_2 = 100, PG_2 = 72, PG_3 = 60$.

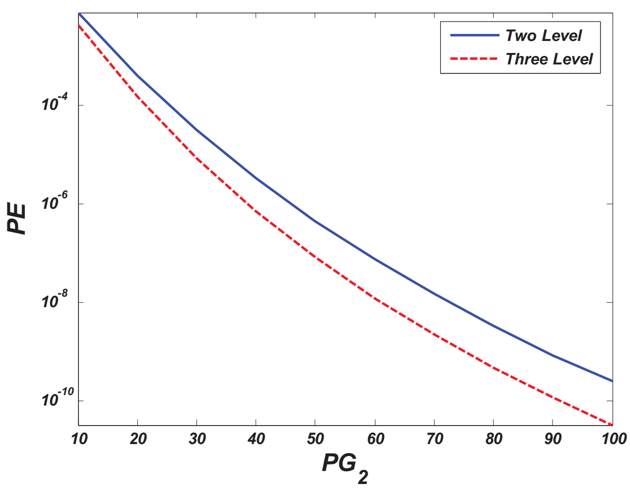

Fig. 9. $PE_{two-level}$ and $PE_{three-level}$ versus PG_2 for $c_1 = 0.8, c_2 = 100, PG_1 = 0.5, PG_3 = 60$.

values of c_1, we can reach a high gain by using three-level codes. Fig. 7 shows that in the case of weak interference $(c_2 \rightarrow 0)$ we just have a small improvement by using three-level codes. But for the condition of strong interference $(c_2 \rightarrow \infty)$ which could be encountered more frequently in UWB applications, we can obtain a very high performance. This is due to the fact that in this region by using three-level codes we can completely remove the interferences effects and thus PE will be independent of the strength of the interferences. In this figure for regions approximately given by $1 \leq c_2 \leq 2$, we have $PE_{two-level} \leq PE_{three-level}$. This phenomenon is due the fact that in calculating $L_{zero,optimum}$ we have used $SNR_{three-level}$ as an approximate measure instead of the desirable parameter $PE_{three-level}$.

Figs. 8, 9 and 10 show that using the three-level codes are actually equivalent in increasing the effective value of each processing gains, i.e., PG_1, PG_2, PG_3. This is surprising, since in three-level codes we actually decrease the use of the available bandwidth but the result indicates a better performance. The rational behind this is that by proper investment on better frequency bands or slots, rather than using all the

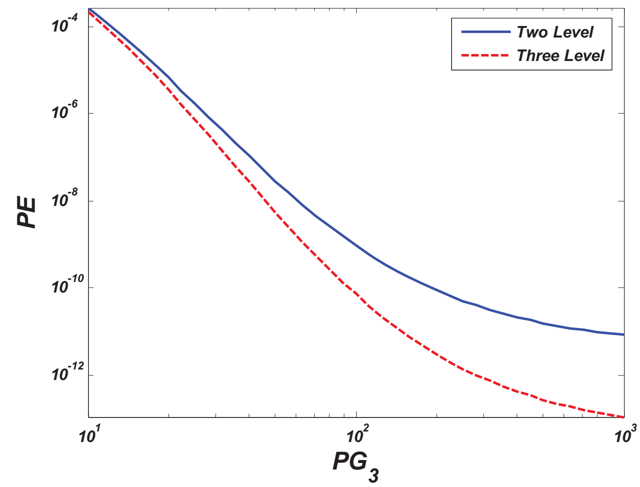

Fig. 10. $PE_{two-level}$ and $PE_{three-level}$ versus PG_3 for $c_1 = 0.8, c_2 = 100, PG_1 = 0.5, PG_2 = 72$.

available bandwidth, we can obtain more effective processing gain and thus a decrease in PE.

VI. Conclusions

In this paper we elaborated on receiver structures that can simultaneously support multiple-access capabilities while reducing the effect of multiple Gaussian interferences using UWB spectrally-encoded ST technique. Central to these structures is the use of a RAKE with $L \times K$ parallel correlator each with a proper weighting factor prior to combining. We introduced a strategy based on a constant average power criterion by using the concept of three-level codes. We showed that using this novel scheme we can further reduce the probability of error. In order to give a deep insight into the behavior of the above structures we discussed an important but yet a simple example and showed that the final results are completely specified through five simple and meaningful parameters. Finally, we would like to highlight that using three-level codes under the assumption of constant average power, may lead to the increase in power content of our transmitted signal on some frequency slots beyond the FCC enforced rules. Indeed this issue, which critically depends on the special problem under consideration, should also be properly considered in a real design procedure.

Appendix A
Establishing Equation (5)

From (1)–(4) we have (A-1) (see next page). But with the help of Fourier transformation properties we can write (A-2) (see next page).

Because of disjoint frequency bands, the above value is equal to zero for any $l \neq \widehat{l}$. For $l = \widehat{l}$, it simplifies to (A-3) (see next page), where for the above equation $E_{\widehat{l}} = \int_{-\infty}^{+\infty} \left| p_{rec}^{\widehat{l}}(t) \right|^2 dt = \int_{-\infty}^{+\infty} \left| p_{rec}^{\widehat{l}}(f) \right|^2 df = \int_{f_{\widehat{l}}-\frac{\Omega}{2}}^{f_{\widehat{l}}+\frac{\Omega}{2}} \left| H(f) \right|^2 df$. It should be obvious that, for all practical purposes, in a CDMA system the applied approximation is valid and is equivalent in using multiple-access codes with large enough length. Now

$$
\begin{aligned}
&\int_{-\infty}^{+\infty} r_{rec}^{(n)}(t) \times \left[\xi_{\hat{l}}^{(1)} \exp\left(-j\theta_{\hat{l},\hat{k}}^{(1,0)}\right) p_{rec}^{(\hat{l})*}\left(t-\tau_{\hat{l},\hat{k}}^{(1,0)}\right)\right] dt \\
&= \sum_{m}\sum_{l=1}^{L}\sum_{k=1}^{K} d_m^{(n)} \xi_l^{(n)} \xi_{\hat{l}}^{(1)} \alpha_{l,k}^{(n,m)} \exp\left(j\theta_{l,k}^{(n,m)}\right) \exp\left(-j\theta_{\hat{l},\hat{k}}^{(1,0)}\right) \\
&\int_{-\infty}^{+\infty} p_{rec}^{(l)}\left(t-mT_b-\tau_n-\tau_{l,k}^{(n,m)}\right) p_{rec}^{(\hat{l})*}\left(t-\tau_{\hat{l},\hat{k}}^{(1,0)}\right) dt
\end{aligned} \tag{A-1}
$$

$$
\begin{aligned}
&\int_{-\infty}^{+\infty} p_{rec}^{(l)}\left(t-mT_b-\tau_n-\tau_{l,k}^{(n,m)}\right) p_{rec}^{(\hat{l})*}\left(t-\tau_{\hat{l},\hat{k}}^{(1,0)}\right) dt \\
&= \int_{-\infty}^{+\infty} p_{rec}^{(l)}(f)\, p_{rec}^{(\hat{l})*}(f) \exp\left(-j2\pi f\left[mT_b+\tau_n+\tau_{l,k}^{(n,m)}-\tau_{\hat{l},\hat{k}}^{(1,0)}\right]\right) df
\end{aligned} \tag{A-2}
$$

$$
\begin{aligned}
&\int_{-\infty}^{+\infty} p_{rec}^{(\hat{l})}(f)\, p_{rec}^{(\hat{l})*}(f) \exp\left(-j2\pi f\left[mT_b+\tau_n+\tau_{\hat{l},k}^{(n,m)}-\tau_{\hat{l},\hat{k}}^{(1,0)}\right]\right) df \\
&= \int_{f_{\hat{l}}-\frac{\Omega}{2}}^{f_{\hat{l}}+\frac{\Omega}{2}} |H(f)|^2 \exp\left(-j2\pi f\left[mT_b+\tau_n+\tau_{\hat{l},k}^{(n,m)}-\tau_{\hat{l},\hat{k}}^{(1,0)}\right]\right) df \\
&\cong E_{\hat{l}} \times \frac{\sin \pi\Omega\left(mT_b+\tau_n+\tau_{\hat{l},k}^{(n,m)}-\tau_{\hat{l},\hat{k}}^{(1,0)}\right)}{\pi\Omega\left(mT_b+\tau_n+\tau_{\hat{l},k}^{(n,m)}\tau_{\hat{l},\hat{k}}^{(1,0)}\right)} \exp\left(-j2\pi f_{\hat{l}}\left[mT_b+\tau_n+\tau_{\hat{l},k}^{(n,m)}-\tau_{\hat{l},\hat{k}}^{(1,0)}\right]\right)
\end{aligned} \tag{A-3}
$$

we consider two different cases: $n=1$ and $n \neq 1$. For $n=1$, using the fact that for all l and n, $\xi_l^{(n)} \times \xi_l^{(n)} = 1$, we can simplify (A-1) with the help of (A-3) as (A-4).

Equation (A-4) consists of three different terms: the first term is the desired term which contains the transmitted bit $d_0^{(1)}$, the second term is due to multipath, and the third term is the intersymbol interference (ISI) term. In order to minimize ISI, it is necessary to select $1 < \Omega T_b$. Under this condition, the ISI term is sufficiently small and thus can be safely ignored. Now, if we define (A-5) (see next page), then we can write (A-4) as (A-6) (see next page), where $n_{\hat{l},\hat{k}}^{MPI}$ is a zero-mean random variable with $\mathbf{E}\left(\left|n_{\hat{l},\hat{k}}^{MPI}\right|^2\right) = E_{\hat{l}}^2 \sum_{\substack{k=1\\k\neq\hat{k}}}^{K} \eta_k \eta'_{k,\hat{k}}$, in which $\eta_k = \mathbf{E}\left(\alpha_{l,k}^{(n,m)}\right)^2$ is the variance of a zero-mean fading coefficient $\alpha_{l,k}^{(n,m)}$, and $\eta'_{k,\hat{k}} = \mathbf{E}\left(\frac{\sin \pi\Omega\left(\tau_{\hat{l},k}^{(1,0)}-\tau_{\hat{l},\hat{k}}^{(1,0)}\right)}{\pi\Omega\left(\tau_{\hat{l},k}^{(1,0)}-\tau_{\hat{l},\hat{k}}^{(1,0)}\right)}\right)$. In defining η_k and $\eta'_{k,\hat{k}}$, we assume that fading parameters, i.e., $\alpha_{l,k}^{(n,m)}$, $\tau_{l,k}^{(n,m)}$ and $\theta_{l,k}^{(n,m)}$, have the same distributions over various l, n and m and the only possible difference is due to different paths from transmitter to the receiver.

In a similar manner for $n \neq 1$, (A-1) reduces to (A-7) (see next page). Therefore, we can define (A-8) (see next page). $n_{\hat{l},\hat{k}}^{MAI}$ is also a zero-mean random variable with $\mathbf{E}\left(\left|n_{\hat{l},\hat{k}}^{MAI}\right|^2\right) = 2(N-1)E_{\hat{l}}^2 \sum_{k=1}^{K} \eta_k \eta''_{k,\hat{k}}$ in which $\eta''_{k,\hat{k}} = \mathbf{E}\left(\frac{\sin \pi\Omega\left(\tau_n+\tau_{\hat{l},k}^{(1,0)}-\tau_{\hat{l},\hat{k}}^{(1,0)}\right)}{\pi\Omega\left(\tau_n+\tau_{\hat{l},k}^{(1,0)}-\tau_{\hat{l},\hat{k}}^{(1,0)}\right)}\right)^2$. We can follow this approach and define (A-9) and (A-10) (see next page), where $n_{\hat{l},\hat{k}}^{GI}$ and $n_{\hat{l},\hat{k}}^{GI}$ are zero-mean Gaussian random variables with $\mathbf{E}\left(\left|n_{\hat{l},\hat{k}}^{GI}\right|^2\right) = N_{\hat{l}}^{GI} E_{\hat{l}}$ and $\mathbf{E}\left(\left|n_{\hat{l},\hat{k}}^{AWGN}\right|^2\right) = N_0 E_{\hat{l}}$. Finally, using (3), (4), (A-6), (A-8), (A-9) and (A-10) we can obtain (5).

APPENDIX B
APPROXIMATIONS ON $\eta'_{k,\hat{k}}$ AND $\eta''_{k,\hat{k}}$

If we consider T_{ds} as the delay spread of the channel, then $\tau_{l,k}^{(n,m)}$s have distribution on $[0, T_{ds}/K]$ and thus

$$
\left(\frac{\sin(\pi\Omega T_{ds}/K)}{\pi\Omega T_{ds}/K}\right)^2 \leq \eta'_{k,\hat{k}} \leq 1 \tag{B-1}
$$

Similarly, since we assume the range over which $\tau_{l,k}^{(n,m)}$ variations is much less than τ_n, i.e., $T_{ds}/K \ll T_b$, then (B-2) (see next page). Therefore, we can approximate $\eta'_{k,\hat{k}}$ and $\eta''_{k,\hat{k}}$ with their worst case limits as $\eta'_{k,\hat{k}} \cong 1$ and $\eta''_{k,\hat{k}} \cong \frac{1}{2\Omega T_b}$. It is obvious that this approximation is pessimistic and thus gives an upper bound value on the actual PE.

$$\begin{aligned}
&\int_{-\infty}^{+\infty} r_{rec}^{(1)}(t) \times \left[\xi_{\hat{l}}^{(1)} \exp\left(-j\theta_{\hat{l},\hat{k}}^{(1,0)}\right) p_{rec}^{(\hat{l})*}\left(t-\tau_{\hat{l},\hat{k}}^{(1,0)}\right)\right] dt \\
&= \sum_m \sum_{k=1}^{K} d_m^{(1)} \alpha_{\hat{l},k}^{(1,m)} E_{\hat{l}} \frac{\sin \pi\Omega\left(mT_b+\tau_{\hat{l},k}^{(1,m)}-\tau_{\hat{l},\hat{k}}^{(1,0)}\right)}{\pi\Omega\left(mT_b+\tau_{\hat{l},k}^{(1,m)}-\tau_{\hat{l},\hat{k}}^{(1,0)}\right)} \exp\left(j\theta_{\hat{l},k}^{(1,m)}-j\theta_{\hat{l},\hat{k}}^{(1,0)}-j2\pi f_{\hat{l}}\left[mT_b+\tau_{\hat{l},k}^{(1,m)}-\tau_{\hat{l},\hat{k}}^{(1,0)}\right]\right) \\
&= d_0^{(1)} \alpha_{\hat{l},\hat{k}}^{(1,0)} E_{\hat{l}} + \sum_{\substack{k=1\\k\neq\hat{k}}}^{K} d_0^{(1)} \alpha_{\hat{l},k}^{(1,0)} E_{\hat{l}} \frac{\sin \pi\Omega\left(\tau_{\hat{l},k}^{(1,0)}-\tau_{\hat{l},\hat{k}}^{(1,0)}\right)}{\pi\Omega\left(\tau_{\hat{l},k}^{(1,0)}-\tau_{\hat{l},\hat{k}}^{(1,0)}\right)} \exp\left(j\theta_{\hat{l},k}^{(1,0)}-j\theta_{\hat{l},\hat{k}}^{(1,0)}-j2\pi f_{\hat{l}}\left[\tau_{\hat{l},k}^{(1,0)}-\tau_{\hat{l},\hat{k}}^{(1,0)}\right]\right) \\
&+\sum_{m\neq 0} \sum_{k=1}^{K} d_m^{(1)} \alpha_{\hat{l},k}^{(1,m)} E_{\hat{l}} \frac{\sin \pi\Omega\left(mT_b+\tau_{\hat{l},k}^{(1,m)}-\tau_{\hat{l},\hat{k}}^{(1,0)}\right)}{\pi\Omega\left(mT_b+\tau_{\hat{l},k}^{(1,m)}-\tau_{\hat{l},\hat{k}}^{(1,0)}\right)} \exp\left(j\theta_{\hat{l},k}^{(1,m)}-j\theta_{\hat{l},\hat{k}}^{(1,0)}-j2\pi f_{\hat{l}}\left[mT_b+\tau_{\hat{l},k}^{(1,m)}-\tau_{\hat{l},\hat{k}}^{(1,0)}\right]\right) \quad \text{(A-4)}
\end{aligned}$$

$$n_{\hat{l},\hat{k}}^{MPI} = \sum_{\substack{k=1\\k\neq\hat{k}}}^{K} d_0^{(1)} \alpha_{\hat{l},k}^{(1,0)} E_{\hat{l}} \frac{\sin \pi\Omega\left(\tau_{\hat{l},k}^{(1,0)}-\tau_{\hat{l},\hat{k}}^{(1,0)}\right)}{\pi\Omega\left(\tau_{\hat{l},k}^{(1,0)}-\tau_{\hat{l},\hat{k}}^{(1,0)}\right)} \exp\left(j\theta_{\hat{l},k}^{(1,0)}-j\theta_{\hat{l},\hat{k}}^{(1,0)}-j2\pi f_{\hat{l}}\left[\tau_{\hat{l},k}^{(1,0)}-\tau_{\hat{l},\hat{k}}^{(1,0)}\right]\right) \quad \text{(A-5)}$$

$$\int_{-\infty}^{+\infty} r_{rec}^{(1)}(t) \times \left[\xi_{\hat{l}}^{(1)} \exp\left(-j\theta_{\hat{l},\hat{k}}^{(1,0)}\right) p_{rec}^{(\hat{l})*}\left(t-\tau_{\hat{l},\hat{k}}^{(1,0)}\right)\right] dt = d_0^{(1)} \alpha_{\hat{l},\hat{k}}^{(1,0)} E_{\hat{l}} + n_{\hat{l},\hat{k}}^{MPI} \quad \text{(A-6)}$$

$$\begin{aligned}
&\int_{-\infty}^{+\infty} r_{rec}^{(n)}(t) \times \left[\xi_{\hat{l}}^{(1)} \exp\left(-j\theta_{\hat{l},\hat{k}}^{(1,0)}\right) p_{rec}^{(\hat{l})*}\left(t-\tau_{\hat{l},\hat{k}}^{(1,0)}\right)\right] dt \\
&= \sum_m \sum_{k=1}^{K} d_m^{(n)} \xi_{\hat{l}}^{(n)} \xi_{\hat{1}}^{(1)} \alpha_{\hat{l},k}^{(n,m)} E_{\hat{l}} \frac{\sin \pi\Omega\left(mT_b+\tau_n+\tau_{\hat{l},k}^{(n,m)}-\tau_{\hat{l},\hat{k}}^{(1,0)}\right)}{\pi\Omega\left(mT_b+\tau_n+\tau_{\hat{l},k}^{(n,m)}-\tau_{\hat{l},\hat{k}}^{(1,0)}\right)} \\
&\quad \times \exp\left(j\theta_{\hat{l},k}^{(n,m)}-j\theta_{\hat{l},\hat{k}}^{(1,0)}-j2\pi f_{\hat{l}}\left[mT_b+\tau_n+\tau_{\hat{l},k}^{(n,m)}-\tau_{\hat{l},\hat{k}}^{(1,0)}\right]\right) \\
&= d_0^{(n)} \sum_{k=1}^{K} \xi_{\hat{l}}^{(n)} \xi_{\hat{l}}^{(1)} \alpha_{\hat{l},k}^{(n,0)} E_{\hat{l}} \frac{\sin \pi\Omega\left(\tau_n+\tau_{\hat{l},k}^{(n,0)}-\tau_{\hat{l},\hat{k}}^{(1,0)}\right)}{\pi\Omega\left(\tau_n+\tau_{\hat{l},k}^{(n,0)}-\tau_{\hat{l},\hat{k}}^{(1,0)}\right)} \exp\left(j\theta_{\hat{l},k}^{(n,0)}-j\theta_{\hat{l},\hat{k}}^{(1,0)}-j2\pi f_{\hat{l}}\left[\tau_n+\tau_{\hat{l},k}^{(n,0)}-\tau_{\hat{l},\hat{k}}^{(1,0)}\right]\right) \\
&\quad + d_{-1}^{(n)} \sum_{k=1}^{K} \xi_{\hat{l}}^{(n)} \xi_{\hat{l}}^{(1)} \alpha_{\hat{l},k}^{(n,-1)} E_{\hat{l}} \frac{\sin \pi\Omega\left(\tau_n-T_b+\tau_{\hat{l},k}^{(n,-1)}-\tau_{\hat{l},\hat{k}}^{(1,0)}\right)}{\pi\Omega\left(\tau_n-T_b+\tau_{\hat{l},k}^{(n,-1)}-\tau_{\hat{l},\hat{k}}^{(1,0)}\right)} \\
&\quad \times \exp\left(j\theta_{\hat{l},k}^{(n,-1)}-j\theta_{\hat{l},\hat{k}}^{(1,0)}-j2\pi f_{\hat{l}}\left[\tau_n-T_b+\tau_{\hat{l},k}^{(n,-1)}-\tau_{\hat{l},\hat{k}}^{(1,0)}\right]\right) \quad \text{(A-7)}
\end{aligned}$$

$$\begin{aligned}
n_{\hat{l},\hat{k}}^{MAI} &= \int_{-\infty}^{+\infty} \sum_{n=2}^{N} r_{rec}^{(n)}(t) \times \left[\xi_{\hat{l}}^{(1)} \exp\left(-j\theta_{\hat{l},\hat{k}}^{(1,0)}\right) p_{rec}^{(\hat{l})*}\left(t-\tau_{\hat{l},\hat{k}}^{(1,0)}\right)\right] dt \\
&= \sum_{n=2}^{N} \sum_{k=1}^{K} d_0^{(n)} \xi_{\hat{l}}^{(n)} \xi_{\hat{l}}^{(1)} \alpha_{\hat{l},k}^{(n,0)} E_{\hat{l}} \frac{\sin \pi\Omega\left(\tau_n+\tau_{\hat{l},k}^{(n,0)}-\tau_{\hat{l},\hat{k}}^{(1,0)}\right)}{\pi\Omega\left(\tau_n+\tau_{\hat{l},k}^{(n,0)}-\tau_{\hat{l},\hat{k}}^{(1,0)}\right)} \exp\left(j\theta_{\hat{l},k}^{(n,0)}-j\theta_{\hat{l},\hat{k}}^{(1,0)}-j2\pi f_{\hat{l}}\left[\tau_n+\tau_{\hat{l},k}^{(n,0)}-\tau_{\hat{l},\hat{k}}^{(1,0)}\right]\right) \\
&+ \sum_{n=2}^{N} \sum_{k=1}^{K} d_{-1}^{(n)} \xi_{\hat{l}}^{(n)} \xi_{\hat{l}}^{(1)} \alpha_{\hat{l},k}^{(n,-1)} E_{\hat{l}} \frac{\sin \pi\Omega\left(\tau_n-T_b+\tau_{\hat{l},k}^{(n,-1)}-\tau_{\hat{l},\hat{k}}^{(1,0)}\right)}{\pi\Omega\left(\tau_n-T_b+\tau_{\hat{l},k}^{(n,-1)}-\tau_{\hat{l},\hat{k}}^{(1,0)}\right)} \\
&\quad \times \exp\left(j\theta_{\hat{l},k}^{(n,-1)}-j\theta_{\hat{l},\hat{k}}^{(1,0)}-j2\pi f_{\hat{l}}\left[\tau_n-T_b+\tau_{\hat{l},k}^{(n,-1)}-\tau_{\hat{l},\hat{k}}^{(1,0)}\right]\right) \quad \text{(A-8)}
\end{aligned}$$

$$\begin{aligned} n_{\widehat{l},\widehat{k}}^{GI} &= \int_{-\infty}^{+\infty} \sum_{l=1}^{L} J_l(t) \times \left[\xi_{\widehat{l}}^{(1)} \exp\left(-j\theta_{\widehat{l},\widehat{k}}^{(1,0)}\right) p_{rec}^{(\widehat{l})*}\left(t-\tau_{\widehat{l},\widehat{k}}^{(1,0)}\right)\right] dt \\ &= \int_{-\infty}^{+\infty} J_{\widehat{l}}(t) \times \left[\xi_{\widehat{l}}^{(1)} \exp\left(-j\theta_{\widehat{l},\widehat{k}}^{(1,0)}\right) p_{rec}^{(\widehat{l})*}\left(t-\tau_{\widehat{l},\widehat{k}}^{(1,0)}\right)\right] dt \end{aligned} \tag{A-9}$$

$$n_{\widehat{l},\widehat{k}}^{AWGN} = \int_{-\infty}^{+\infty} n(t) \times \left[\xi_{\widehat{l}}^{(1)} \exp\left(-j\theta_{\widehat{l},\widehat{k}}^{(1,0)}\right) p_{rec}^{(\widehat{l})*}\left(t-\tau_{\widehat{l},\widehat{k}}^{(1,0)}\right)\right] dt \tag{A-10}$$

$$\eta''_{k,\widehat{k}} \cong \frac{1}{T_b}\int_0^{T_b}\left(\frac{\sin(\pi\Omega\tau)}{\pi\Omega\tau}\right)^2 d\tau \le \frac{1}{T_b}\int_0^{\infty}\left(\frac{\sin(\pi\Omega\tau)}{\pi\Omega\tau}\right)^2 d\tau = \frac{1}{2\Omega T_b} \tag{B-2}$$

$$\begin{aligned} \mathbf{E}(\exp(s\times\gamma_1)) &= \prod_{\widehat{l}=1}^{L-L_{GI}} \prod_{\widehat{k}=1}^{K}\left(1-\left[\frac{E}{L}\left(1+\frac{N-1}{\Omega T_b}\right)\sum_{k=1}^{K}\eta_k+N_0\right]^{-1}\times\frac{2\rho E}{L}\times s\right)^{-\mu_k} \\ &= \left(1-\left[\frac{E}{L}\left(1+\frac{N-1}{\Omega T_b}\right)\sum_{k=1}^{K}\eta_k+N_0\right]^{-1}\times\frac{2\rho E}{L}\times s\right)^{-(L-L_{GI})\sum_{k=1}^{K}\mu_k} \\ &= (1-\rho\rho_1 s)^{-(L-L_{GI})\sum_{k=1}^{K}\mu_k} \end{aligned} \tag{C-1}$$

$$P(\gamma_1) = \frac{1/\gamma_1}{\Gamma\left((L-L_{GI})\sum_{k=1}^{K}\mu_k\right)} \times (\gamma_1/\rho\rho_1)^{(L-L_{GI})\sum_{k=1}^{K}\mu_k} \times \exp(-\gamma_1/\rho\rho_1) \tag{C-2}$$

$$\begin{aligned} P(\gamma_2) &= \frac{1/\gamma_2}{\Gamma\left(L_{GI}\sum_{k=1}^{K}\mu_k\right)} \times (\gamma_2/\rho\rho_2)^{L_{GI}\sum_{k=1}^{K}\mu_k} \times \exp(-\gamma_2/\rho\rho_2) \\ P(\gamma'_1) &= \frac{1/\gamma'_1}{\Gamma\left((L-L_{GI})\sum_{k=1}^{K}\mu_k\right)} \times (\gamma'_1/\rho\rho'_1)^{(L-L_{GI})\sum_{k=1}^{K}\mu_k} \times \exp(-\gamma'_1/\rho\rho'_1) \\ P(\gamma'_2) &= \frac{1/\gamma'_2}{\Gamma\left((L-L_{zero})\sum_{k=1}^{K}\mu_k\right)} \times (\gamma'_2/\rho\rho'_2)^{(L_{GI}-L_{zero})\sum_{k=1}^{K}\mu_k} \times \exp(-\gamma'_2/\rho\rho'_2) \end{aligned} \tag{C-3}$$

$$\begin{aligned} \rho_2 &= \frac{2E}{L}\times\left[\frac{E}{L}\left(1+\frac{N-1}{\Omega T_b}\right)\sum_{k=1}^{K}\eta_k+N_{GI}+N_0\right]^{-1} \\ \rho'_1 &= \frac{2E}{L}\times\left[\frac{E}{L}\left(1+\frac{N-1}{\Omega T_b}\right)\sum_{k=1}^{K}\eta_k+N_0\times(1-L_{zero}/L)\right]^{-1} \\ \rho'_2 &= \frac{2E}{L}\times\left[\frac{E}{L}\left(1+\frac{N-1}{\Omega T_b}\right)\sum_{k=1}^{K}\eta_k+(N_{GI}+N_0)\times(1-L_{zero}/L)\right]^{-1} \end{aligned} \tag{C-4}$$

APPENDIX C
DISTRIBUTION OF γ_1, γ_2, γ_1' AND γ_2'

Under the conditions of our example and similar to (10), we can write (C-1), in which $\rho_1 = \frac{2E}{L} \times \left[\frac{E}{L}\left(1+\frac{N-1}{\Omega T_b}\right)\sum_{k=1}^{K}\eta_k + N_0\right]^{-1}$. Therefore, γ_1 has Gamma distribution and so (C-2). Similar arguments yield (C-3) and (C-4).

REFERENCES

[1] J. A. Salehi, A. M. Weiner, and J. P. Heritage, "Coherent ultrashort light pulse code-division multiple access communication systems," *IEEE J. Lightwave Technol.*, vol. 8., pp. 478–491, Mar. 1990.

[2] C. R. C. M. da Silva and L. B. Milstein, "Spectral-encoded UWB communication systems: Real-time implementation and interference suppression," *IEEE Trans. Commun.*, vol. 53, pp. 1391–1401, Aug. 2005.

[3] C. R. C. M. da Silva and L. B. Milstein, "The effect of narrowband interference on UWB communication systems with imperfect channel estimation," *IEEE J. Select. Areas Commun.*, vol. 24, pp. 717–723, Apr. 2006.

[4] M. Farhang and J. A. Salehi, "Spread-time/time-hopping UWB CDMA communication," in *Proc. IEEE International Symp. Commun. Inform. Technol.*, Oct. 2004, vol. 2, pp. 1047–1050.

[5] P. M. Crespo, M. L. Honig, and J. A. Salehi, "Spread-time code division multiple access," *IEEE Trans. Commun.*, vol. 43, pp. 2139–2148, June 1995.

[6] M. G. Shayesteh, J. A. Salehi, and M. Nasiri-Kenari, "Spread-time CDMA resistance in fading channels," *IEEE Trans. Wireless Commun.*, vol. 2, no. 3, pp. 446–458, May 2003.

[7] J. Wang and L. B. Milstein, "Multicarrier CDMA overlay for ultra-wideband communications," IEEE *Trans. Commun.*, vol. 52, pp. 1664–1669, Oct. 2004.

[8] L. Bomer and M. Antweiler, "Perfect three-level and three-phase sequences and arrays," *IEEE Trans. Commun.*, vol. 42, pp. 767–772, Feb.-Apr. 1994.

[9] X. Chu and R. D. Murch, "The effect of NBI on time-hopping systems," *IEEE Trans. Wireless Commun.*, vol. 3, no. 5, pp. 1431–1436, Sep. 2004.

[10] M. Z. Win and R. A. Scholtz, "Ultra-wide bandwidth time-hopping spread-spectrum impulse radio for wireless multiple-access communications," *IEEE J. Select. Areas Commun.*, vol. 20, pp.1613–1627, Dec. 2002.

[11] R. A. Scholtz, R. Weaver, E. Homier, J. Lee, P. Hilmes, A. Taha, and R. Wilson, "UWB radio deployment challenges," in *Proc. 11th IEEE International Symposium Personal, Indoor Mobile Radio Commun.*, vol. 1,2000, pp. 620–625.

[12] R. K. Mallik, M. Z. Win, M. Chiani, and A. Zanella, "Bit-error probability for optimum combining of binary signals in the presence of interference and noise," *IEEE Trans. Commun.*, vol. 3, no. 2, pp. 395–407, Mar. 2004.

[13] M. Chiani, M. Z. Win, and A. Zanella, "Error probability for optimum combining of *M*-ary PSK signals in the presence of interference and noise" *IEEE Trans. Commun.*, vol. 51, no. 11, pp.1949–1957, Nov. 2003.

Saeed Mashhadi was born on January 1981, in Tafresh, Iran. He received the B.S. and M.S. degrees with honors all in electrical engineering from Sharif University of Technology (SUT), Tehran, Iran, in 2002 and 2004, respectively. He is currently working toward the PhD degree in the Department of Electrical Engineering at Sharif University. Since 2003, he has been a member of the Optical Networks Research Laboratory (ONRL) at SUT. His research interests are in the areas of optical multiaccess networks, in particular, fiber-optic CDMA, wireless spread-time CDMA, and information theory. Mr. Mashhadi is a recipient of the Gold Medal of the Iranian Olympiad in Electrical Engineering.

Jawad A. Salehi (M'02, S'06) was born in Kazemain, Iraq, on December 22, 1956. He received the B.S. degree in electrical engineering from the University of California, Irvine, in 1979, and the M.S. and Ph.D. degrees, all in electrical engineering, from the University of Southern California (USC), Los Angeles, in 1980 and 1984, respectively. From 1981 to 1984, he was a full-time Research Assistant at the Communication Science Institute at USC, where he was engaged in research in the area of spread spectrum systems. From 1984 to 1993, he was a Member of Technical Staff of the Applied Research Area, Bell Communications Research (Bellcore), Morristown, NJ. From February to May 1990, he was with the Laboratory of Information and Decision Systems, Massachusetts Institute of Technology (MIT), Cambridge, as a Visiting Research Scientist conducting research on optical multiple-access networks. He was an Associate Professor from 1997 to 2003 and is currently a Full Professor with the Electrical Engineering (EE) Department, Sharif University of Technology (SUT), Tehran, Iran. From 1999 to 2001, he was the Head of Mobile Communications Systems Group and Codirector of Advanced and Wideband Code Division Multiple Access (CDMA) Laboratory at Iran Telecom Research Center (ITRC), Tehran, conducting research in the area of advance CDMA techniques for optical and radio communications systems. From 2003 to 2006 he was the director of the National Center of Excellence in Communications Science at the EE department of SUT. In 2003, he founded and directed the Optical Networks Research Laboratory (ONRL), Electrical Engineering Department, SUT, for advanced theoretical and experimental research in futuristic all-optical networks. He is also a Cofounder of Advanced Communications Research Institute (ACRI) at SUT for advancing the graduate school research program in communications science. His current research interests include optical multiaccess networks, in particular, optical orthogonal codes (OOC); fiber-optic CDMA; femtosecond or ultra-short light pulse CDMA; spread time CDMA; holographic CDMA; wireless indoor optical CDMA; all-optical synchronization; and applications of erbium-doped fiber amplifiers (EDFAs) in optical systems. He is the holder of 12 U.S. patents on optical CDMA. Dr. Salehi is a Recipient of Bellcore's Award of Excellence, the Outstanding Research Award of the EE Department of SUT in 2002, 2003, and 2006, the Outstanding Research Award of SUT in 2003, the Nationwide Outstanding Research Award from the Ministry of Higher Education in 2003, and the Nation's Highly Cited Researcher Award 2004. In 2007 he received the first prize in fundamental research from Khwarizmi International Prize, Tehran, Iran and he also received Outstanding Inventor Award (Gold Medal) World Intellectual Property Organization (WIPO) Geneva, Switzerland. Recently, he was introduced as among the 250 preeminent and most influential researchers worldwide by the Institute for Scientific Information (ISI), Highly Cited in the computer-science category. He is the Co-recipient of IEEE's Best Paper Award ("Spread-time/time-hopping ultrawideband (UWB) CDMA communications systems") from the International Symposium on Communications and Information Technology, October 2004, Japan. He was a member of the organizing committee for the first and the second IEEE Conference on Neural Information. Since May 2001, he has been serving as an Associate Editor for optical CDMA of the IEEE TRANSACTIONS ON COMMUNICATIONS. In September 2005, he was elected as the interim Chair of the IEEE Iran section.